

A NEW METHODOLOGY TO APPLY ESSENTIAL BOUNDARY CONDITIONS IN MESH-FREE METHODS

Rodrigo Rossi

Universidade de Caxias do Sul, Departamento de Engenharia Mecânica, Cidade Universitária, Caxias do Sul, RS, Brasil, CEP 95070-560.
rossi@ucs.br

Marcelo Krajnc Alves

Universidade Federal de Santa Catarina, Departamento de Engenharia Mecânica, Campus Trindade, Florianópolis, SC, Brasil, CEP 88010-970,
krajnc@grante.ufsc.br

Abstract. *In this work we present a Modified Element-Free Galerkin Method (MEFGM) that allows the imposition of the essential boundary conditions in the same way as in the traditional Finite Element Method. The proposed MEFGM consists in the use of a special weight function at the vicinity where the essential boundary conditions are applied. For those particles that does not rely in such vicinity a traditional mesh-free weight function is employed, as the cubic or quartic splines. The resulting shape functions satisfy the kronecker delta property in the essential boundary, unless by a small perturbation, allowing direct imposition of the essential boundary conditions. Furthermore, as the referred shape functions are constructed with the same intrinsic base the approximation keeps the reproducibility property overall the domain, an important property of the Moving Least Square Approximation. The range of the magnitude of the perturbation parameter is investigated by the analysis of its effect over some elastic plane stress problems with analytical solution.*

Keywords. Mesh-free, EFG, PUFEM, MLSA

1. Introduction

The imposition of the essential boundary conditions in the called mesh-free or meshless methods is one of most important drawbacks of such methodology when compared with the traditional Finite Element Method (FEM). The difficulty to impose the essential boundary conditions appears due to the fact that, in general, the global shape functions, employed in the mesh-free methods, do not represent an interpolation, but an approximation of the field considered. Research has been addressed in the last decade to overlap not only this shortcoming but also some others inherent problematic questions of such method, as for example the development of appropriate numerical integration.

Diverse approaches can be found in the literature to overcome this problem. Among them are the usages of:

- Lagrange Multiplier methods by Belytschko and Lu and Gu (1994);
- Penalty methods by Zhu and Alturi (1998);
- Singular weight functions by Lancaster and Salkauskas (1981) and Duarte and Oden (1996);
- Combination of EFG with FE methods by Belytschko, Organ and Krongauz (1995), Hegen (1996), Krongauz and Belytschko (1996) and Huerta and Méndez (2000);
- Introduction of modified variational forms and other approaches Mukherjee and Mukherjee (1997), Kaljević and Saigal (1997) and Gu and Liu (2001).

All these methodologies have some advantages but also disadvantages. In this work it is presented a modified version of the element-free Galerkin method, Alves and Rossi (2003), which allows the direct enforcement, in some limiting sense, of the essential boundary conditions. This method can be seen as a conventional Element-Free Galerkin (EFG) method, containing a set of different weight functions, which automatically selects at each particle a suitable type of weight function and compute the adequate size of its support. Basically, the method employs a conventional EFG weight function and a weight function derived from an Extended Partition of Unity Finite Element (EPUFE) method, see section 2.4. This EPUFE weight function will only be defined at particles belonging to a neighborhood of the essential boundary. Conventional weight functions, such as quartic splines, will be defined at the remaining particles. In order to perform the integration, control and manage the data objects, we make use of an integration mesh composed by triangular integration cells.

In order to attest the performance of the proposed method we solve some elastic problems subjected to a plane stress condition. The size of the support of the EFG weight functions and the range of the magnitude of the perturbation parameter are investigated considering different integration meshes and number of integration points. In addition, it is also presented some convergence investigations.

2. Approximation method

2.1. Moving least square approximation

The MLSA, Lancaster and Salkauskas (1981), allows us to construct an approximation function $u^h(\mathbf{x})$ that fits a set of discrete data with the use of a weighted least square approximation. The weight function is allowed to move based on

the point at which the approximation is to be determined. The MLSA $u^h(\mathbf{x})$ that fits a set of discrete data $\{u_I, I = 1, \dots, n\}$, is given by:

$$u^h(\mathbf{x}) = \sum_{I=1}^n \Phi_I(\mathbf{x}) u_I \quad (1)$$

where

$$\Phi_I(\mathbf{x}) = \mathbf{p}(\mathbf{x}) \cdot \mathbf{A}(\mathbf{x})^{-1} \mathbf{b}_I(\mathbf{x}) \quad (2)$$

$$\mathbf{A}(\mathbf{x}) = \sum_{I=1}^n w(\mathbf{x} - \mathbf{x}_I) [\mathbf{p}(\mathbf{x}_I) \otimes \mathbf{p}(\mathbf{x}_I)] \quad (3)$$

and

$$\mathbf{b}_I(\mathbf{x}) = w(\mathbf{x} - \mathbf{x}_I) \mathbf{p}(\mathbf{x}_I). \quad (4)$$

Here, $p_j(\mathbf{x})$, $j = 1, \dots, m$ represents the set of base functions employed in the MLSA, $w(\mathbf{x} - \mathbf{x}_I)$ is a weight function centered at \mathbf{x}_I that regulates the influence of how the neighboring points will be considered, $\Phi_I(\mathbf{x})$ is denoted the global shape function and $\mathbf{A}(\mathbf{x})$ is the moment matrix.

2.2. Consistency and partition of unity of an approximation

The order of consistency of an approximation is defined as the order of the arbitrary polynomial field that can be exactly represented by the fitting procedure. Now, since the MLSA is capable of reproducing exactly linear combinations of the base functions in $\mathbf{p}(\mathbf{x})$, we can obtain a consistency condition of order k by using $\mathbf{p}^T(\mathbf{x}) = [1, x, y, x^2, xy, y^2, \dots, x^k, \dots, xy^{k-1}, y^k]$. This consistency condition impose restrictions to the global shape functions which leads, in the linear case, to the following relations:

$$\sum_{I=1}^n \Phi_I(\mathbf{x}) = 1, \quad (5)$$

$$\sum_{I=1}^n \Phi_I(\mathbf{x}) x_I = x \text{ and } \sum_{I=1}^n \Phi_I(\mathbf{x}) y_I = y. \quad (6)$$

According to Eq. (5) the set $\{\Phi_I(\mathbf{x}), I = 1, \dots, n\}$ defines a partition of unity.

The aim of the EFG method is to construct a set of global shape functions, using the MLSA, which defines the approximation space, employed by the Galerkin method. However, a global shape function $\Phi_I(\mathbf{x})$, derived from the MLSA, does not satisfy, in general, the kronecker delta property, i.e., $\Phi_I(\mathbf{x}_J) \neq \delta_{IJ}$. As a consequence, we cannot directly enforce, by prescribing nodal values, the essential boundary conditions. In order to avoid these difficulties, we introduce a modified EFG method that combines the EPUFE method with the conventional EFG method with the objective of imposing, in some limiting sense, the essential boundary conditions.

2.3. Partition of unity finite element method

The global shape functions $\Phi_I(\mathbf{x})$, associated with the classical PUFEM, is obtained as a particularization of the MLSA where we consider a single constant base function, $\mathbf{p}^T(\mathbf{x}) = [1]$, and use a traditional finite element base as the weight function, Melenk and Babuška (1996). A typical support of a PUFEM global shape function is illustrated in Fig (1). Notice that, the adjacent node list of $\mathbf{x}_I = (x_I, y_I)$ is the set $\{\mathbf{x}_1, \mathbf{x}_2, \mathbf{x}_3, \mathbf{x}_4, \mathbf{x}_5\}$. In the particular case, where the partition of the domain employs triangular integration cells and the weight function is given by the classical linear triangular finite element base function, we can derive the following expression for the weight function centered at \mathbf{x}_I :

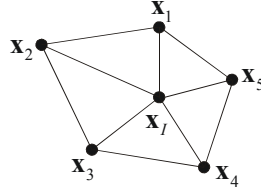


Figure 1. Typical PUFEM support to a triangular integration mesh

$$w(\mathbf{x} - \mathbf{x}_I) = \begin{cases} \frac{1}{2A} [(x_i y_{i+1} - x_{i+1} y_i) + (y_i - y_{i+1})x + (x_{i+1} - x_i)y], & \mathbf{x} \in \text{supp}[\Phi_I(\mathbf{x})], \\ 0, & \text{otherwise} \end{cases}, \quad (7)$$

where \mathbf{x}_i and \mathbf{x}_{i+1} are the elements of the adjacent node list set in a counter clockwise sense, and A is the cell area, given by

$$A = \frac{1}{2} \det \begin{bmatrix} 1 & x_i & y_i \\ 1 & x_i & y_i \\ 1 & x_{i+1} & y_{i+1} \end{bmatrix}. \quad (8)$$

However, the usage of an increased intrinsic base $\mathbf{p}(\mathbf{x})$ together with a PUFEM weight function causes the moment matrix $\mathbf{A}(\mathbf{x})$ to be singular on the boundary of the support of the weight function. In fact, the particle distribution is not arbitrary since it must satisfy a stability condition that is necessary for $\mathbf{A}(\mathbf{x})$ to be regular. The stability condition, Liu and Belytschko (1997), may be stated as:

$$\text{card}\{\mathbf{x}_j | \Phi_j(\mathbf{x}) \neq 0\} \geq \dim[\mathbf{A}(\mathbf{x})]. \quad (9)$$

i.e., the number of particles \mathbf{x}_j , whose associated shape function $\Phi_j(\mathbf{x})$ have a nonzero value at \mathbf{x} , must be larger than the size of $\mathbf{A}(\mathbf{x})$, which is given by the number of base functions in $\mathbf{p}(\mathbf{x})$. Moreover, the particle distribution must be such that, if $\mathbf{x} \in R^n$ then there should be $n+1$ particles whose position vectors form a nonzero n -th rank simplex element.

Hence, in the particular case where $\mathbf{x} \in R^2$ and $\mathbf{p}^T(\mathbf{x}) = [1, x, y]$, we must assure that for all $\mathbf{x} \in \bar{\Omega}$ there must be at least three particles whose weight functions have a nonzero value at \mathbf{x} and whose position vector form a triangle with a non zero area.

2.4. Extended partition of unity finite element method

The objective here is to modify the support of the PUFEM weight function, used in the PUFEM, so that we can satisfy the stability condition for $\mathbf{x} \in R^2$ and $\mathbf{p}^T(\mathbf{x}) = [1, x, y]$. Notice that, since the MLSA reproduces exactly the base functions in $\mathbf{p}(\mathbf{x})$, the consideration of a linear base ensures the satisfaction of the classical patch test, normally verified in the FEM.

In order to satisfy the stability condition the support of the classical PUFEM weight functions is extended by a given ε as illustrated in Fig (2). This extension assures the regularity of $\mathbf{A}(\mathbf{x})$ and the extended points, shown in Fig. (2), are determined as:

$$\mathbf{x}_i^* = \mathbf{x}_i + \varepsilon(\mathbf{x}_i - \mathbf{x}_I). \quad (10)$$

Now, letting $\varepsilon \rightarrow 0$, we derive a global shape function that satisfy, in the limit, at a given particle \mathbf{x}_j , the kronecker delta property, i.e.,

$$\lim_{\varepsilon \rightarrow 0} \Phi_i(\mathbf{x}_j) = \delta_{ij}. \quad (11)$$

Thus, the essential boundary conditions can be properly enforced, provided we consider a sufficiently small value for ε . A sensitivity analysis of ε is presented in the problem case section.

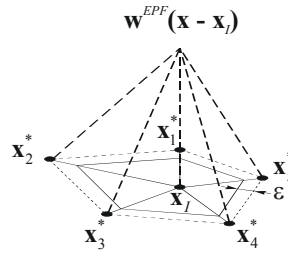


Figure 2. Extended PUFEM support

2.5. Modified element-free Galerkin method

The objective of the modified EFG method is to combine in a suitable way the presented EPUFE and the conventional EFG weight functions so that we can enforce approximately the essential boundary condition by directly prescribing the nodal values, as done by the FEM. Thus the presented method can be seen as a conventional EFG method, having a set of different weight functions, which is able to automatically select, at each particle, the proper type of weight function and to compute the adequate size of its support.

The strategy can be shown by considering a body with domain Ω and boundary $\partial\Omega$, where $\partial\Omega = \Gamma_u \cup \Gamma_t$ and $\Gamma_u \cap \Gamma_t = \emptyset$. Here, Γ_u and Γ_t are respectively the part of $\partial\Omega$ with prescribed essential and natural boundary conditions. Notice that the EPUFE weight functions are specified at particles that belong to a neighborhood of Γ_u and at the remaining particles a conventional EFG weight function is specified.

The advantage of using a conventional EFG weight function relies in the fact that the derived global shape functions depend weakly on the employed integration cell. The same is not true with the FEM. Moreover, if the weight function is continuous together with its first k -derivatives, the derived global shape functions are also continuous together with its first k -derivatives, Belytschko et al (1994).

It is important to notice that the enforcement of the essential boundary condition, by directly prescribing nodal values, can only be accomplished if we assure that there is no overlapping of the support of the conventional EFG weight functions with any part of the boundary Γ_u .

The conventional EFG weight function employed in this work is the quartic spline function, given by:

$$w^{EFG}(r) = \begin{cases} 1 - 6r^2 + 8r^3 - 3r^4, & \text{for } r \leq 1.0 \\ 0, & \text{for } r > 1.0 \end{cases} \quad (12)$$

where $r = r_i / \bar{r}_i$ with $r_i = \|\mathbf{x} - \mathbf{x}_i\|$. The radius \bar{r}_i , defining the support of $w^{EFG}(\mathbf{x})$, is determined, as shown in Fig. (3), by

$$\bar{r}_i = \beta \cdot r_{I_{\max}}, \quad \beta > 1, \quad \beta \in R \quad (13)$$

with

$$r_{I_{\max}} = \max_i \|\mathbf{x}_i - \mathbf{x}_I\|, \quad i \in J_I, \quad (14)$$

where J_I represents the set of adjacent nodes associated with \mathbf{x}_I .

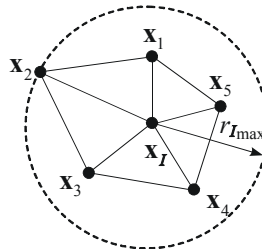


Figure 3. Radius of EFG weight function

2.6. Covering algorithm

The strategy employed in the covering algorithm consists initially in a triangularization of the domain. Once the mesh nodes/particles are defined we may describe the algorithm as:

- For each particle \mathbf{x}_I , do:
 - If ($\mathbf{x}_I \in \Gamma_u$) then
 - Employ at \mathbf{x}_I an EPUFE weight, $w_I^{EPUFE}(\mathbf{x})$.
 - Else
 - Determine the support of the trial $w_I^{EFG}(\mathbf{x})$.
 - (i) Get the adjacent node list set, associated to the particle \mathbf{x}_I
 - (ii) Determine the radius, \bar{r}_I , by Eq.(13), of the support of the trial $w_I^{EFG}(\mathbf{x})$. Compute r_{adm} , by determining the shortest distance from the given particle \mathbf{x}_I to every boundary segment approximating Γ_u , as illustrated in Fig. (4).
 - If ($\bar{r}_I < r_{adm}$) then
 - Employ at \mathbf{x}_I the given trial $w_I^{EFG}(\mathbf{x})$
 - Else
 - Employ at \mathbf{x}_I an $w_I^{EPUFE}(\mathbf{x})$
- End if
- End if
- End do.

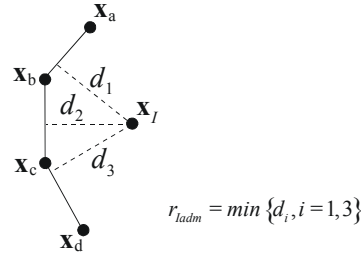


Figure 4. Definition of the admissible radius

At this point it is important to notice that at points $\mathbf{x} \in \Omega$ that are contained only in the support of EPUFE weight functions the resulting approximation is similar to the interpolation obtained by the FEM. Moreover, for points $\mathbf{x} \in \Omega$ that belong only to the support of EFG weight functions, the resulting approximation may have an arbitrary degree of regularity, depending only on the regularity of the selected weight function.

However, at regions whose points $\mathbf{x} \in \Omega$ are contained in both EPUFE and EFG weight functions, the regularity of the resulting approximation is controlled by the regularity of the EPUFE weight function and is non-polynomial. As a consequence, we may experience a loss of accuracy of the solution in this transition region, which is due to numerical integration errors and discontinuities in the stress field.

An example of such covering procedure is illustrated in Fig. (5).

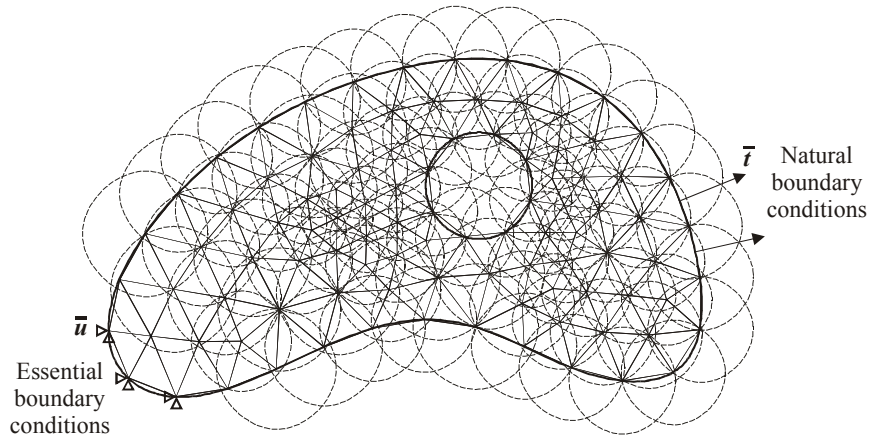


Figure 5. A coverage example of the proposed MEFG.

3. Elastostatics formulation

Let $\Omega \subset \mathbb{R}^2$ be a bounded domain with a Lipschitz boundary $\partial\Omega$, subjected to: a prescribed body force \mathbf{b} defined on Ω , a prescribed surface traction $\bar{\mathbf{t}}$ defined on Γ_t and a prescribed displacement $\mathbf{u} = \bar{\mathbf{u}}$ defined on Γ_u . The classical boundary value problem associated with elastostatics may be stated as: Find \mathbf{u} so that

$$\begin{aligned} \operatorname{div} \boldsymbol{\sigma} + \mathbf{b} &= \mathbf{0}, \quad \forall \mathbf{x} \in \Omega \\ \boldsymbol{\sigma} \mathbf{n} &= \bar{\mathbf{t}}, \quad \forall \mathbf{x} \in \Gamma_t \\ \mathbf{u} &= \bar{\mathbf{u}}, \quad \forall \mathbf{x} \in \Gamma_u \end{aligned} \quad (15)$$

Here, \mathbf{n} is the outer normal to the surface at Γ_t and $\boldsymbol{\sigma}$ is the Cauchy stress tensor with

$$\boldsymbol{\sigma} = \mathbf{D} \boldsymbol{\varepsilon}, \quad (16)$$

where $\boldsymbol{\varepsilon}(\mathbf{u}) = \frac{1}{2} [\nabla(\mathbf{u}) + \nabla(\mathbf{u})^T]$ is the infinitesimal elastic strain tensor and \mathbf{D} is the elastic constitutive relation.

Now, let $H = \{\mathbf{u} | u_i \in H^1(\Omega), \mathbf{u} = \bar{\mathbf{u}} \text{ at } \Gamma_u\}$ denotes the set of admissible displacements and $H_0 = \{\mathbf{u} | u_i \in H^1(\Omega), \mathbf{u} = 0 \text{ at } \Gamma_u\}$ the set of admissible variations. The weak formulation of Eq. (15) may be stated as: Find $\mathbf{u} \in H$ such that

$$a(\mathbf{u}, \mathbf{v}) = L(\mathbf{v}), \quad \forall \mathbf{v} \in H_0 \quad (17)$$

where

$$a(\mathbf{u}, \mathbf{v}) = \int_{\Omega} \boldsymbol{\sigma}(\mathbf{u}) \cdot \boldsymbol{\varepsilon}(\mathbf{v}) d\Omega \quad (18)$$

and

$$L(\mathbf{v}) = \int_{\Omega} \mathbf{b} \cdot \mathbf{v} d\Omega + \int_{\Gamma_t} \bar{\mathbf{t}} \cdot \mathbf{v} d\Gamma. \quad (19)$$

3.1. Error measures norms

Let us first define the norms and the errors for the convergence analysis. The energy norm is defined as

$$\|\mathbf{u}\|_E = a(\mathbf{u}, \mathbf{u})^{1/2}, \quad (20)$$

and the L_2 displacement norm as

$$\|\mathbf{u}\|_{L_2} = \left(\int_{\Omega} \mathbf{u} \cdot \mathbf{u} d\Omega \right)^{1/2}. \quad (21)$$

Now, the relative error measures may be defined as:

$$\eta_E = \frac{\|\mathbf{u} - \mathbf{u}^h\|_E}{\|\mathbf{u}\|_E} \quad \text{and} \quad \eta_{L_2} = \frac{\|\mathbf{u} - \mathbf{u}^h\|_{L_2}}{\|\mathbf{u}\|_{L_2}}, \quad (22)$$

for energy norm and the L_2 norm respectively.

4. Problem cases

In order to investigate the influence of the parameter ε and of the support size β in the proposed method we solve two classical selected problems with analytical solution considering plane stress assumption. Here, for simplicity, we employ a unique material whose properties are: The Young's Modulus $E=210\text{GPa}$ and the Poisson's ratio $\nu=0.3$. Also, we consider two different Gauss-Legendre rules with 7 and 25 integration points.

4.1. Cantilever beam

At this point, we consider the problem illustrated in Fig. (6). In this figure we consider integration meshes that are homogeneously refined. These structured integration meshes will be used in the sensitivity analysis of the parameter ε and for determination of a suitable value for β . The length and the height of the beam are respectively $L=8\text{mm}$, $D=1\text{mm}$ and has a transversal rectangular section with thickness $t=1\text{mm}$. The transversal load is $P=1\text{N}$. The analytical solution, Timoshenko and Goodier (1970), of this problem is given by

$$u_x = \frac{-Py}{6EI} \left[(6L-3x)x + (2+\nu) \left(y^2 - \frac{D^2}{4} \right) \right] \text{ and } u_y = \frac{P}{6EI} \left[3\nu y^2 (L-x) + (4+5\nu) \left(\frac{D^2 x}{4} \right) + (3L-x)x^2 \right] \quad (23)$$

for the displacement components and

$$\sigma_{xx} = \frac{-P(L-x)y}{I}, \quad \sigma_{yy} = 0 \text{ and } \sigma_{xy} = \frac{P}{2I} \left(\frac{D^2}{4} - y^2 \right), \quad (24)$$

for the stress components, where $I = tD^3/12$ is the moment of inertia of the cross section. Here we apply as natural conditions at $x=0$ and $x=L$, the prescribed traction values given by the combination of Eq. (24) and Eq. (15).

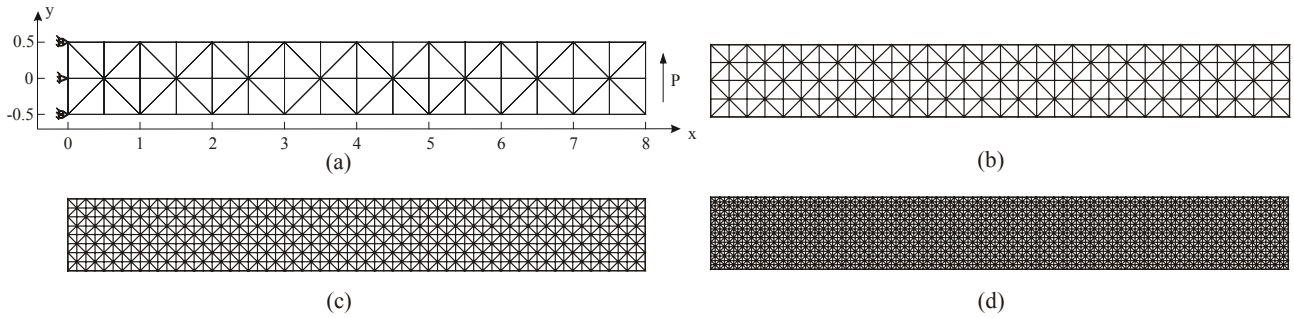
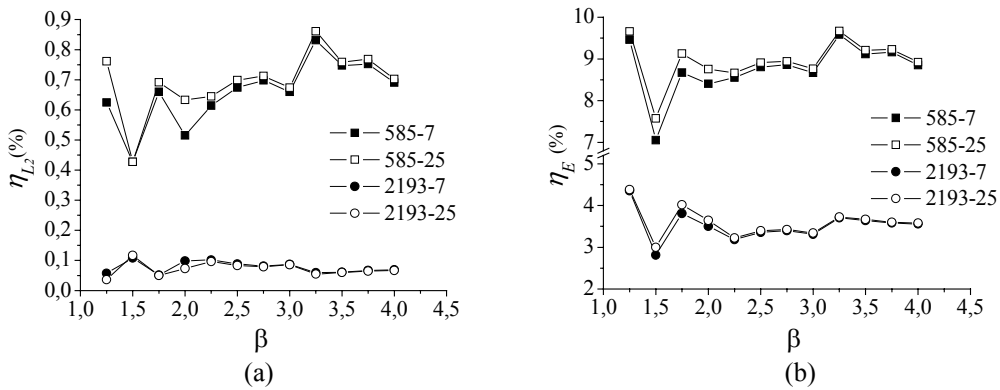


Figure 6. Cantilever beam model problem and integration meshes: a) integration mesh with 64 cells/51 nodes; b) 256 cells/165 nodes; c) 1024 cells/585 nodes; d) 4096 cells/2193 nodes

The first investigation performed is the determination of the support size β . This analysis was performed considering the effect of the change in β upon the norms η_E and η_{L_2} . The integration meshes used in this study were Fig. (6c) and Fig. (6d) and was considering $\varepsilon=10^{-4}$. The results are depicted in Fig. (7a) and Fig. (7b). From these results it is possible conclude that $\beta \cong 1.5$ is a suitable value. Figures (7c) and (7d) shows the sensitivity analyses of the parameter ε with relation to η_E and η_{L_2} , still considering meshes in Fig. (6c) and Fig. (6d) and assuming $\beta=1.5$. Figures (7e), (7f), (7g) and (7h) shows convergence aspects for meshes (6a) to (6d). The legends in the Fig. (7a) to (7d) are the number of particles and number of integration points respectively. Notice that in Fig. (7g) and Fig. (7e), the dashed upper lines represent the exact energy norm and L_2 norm for the proposed cantilever problem.



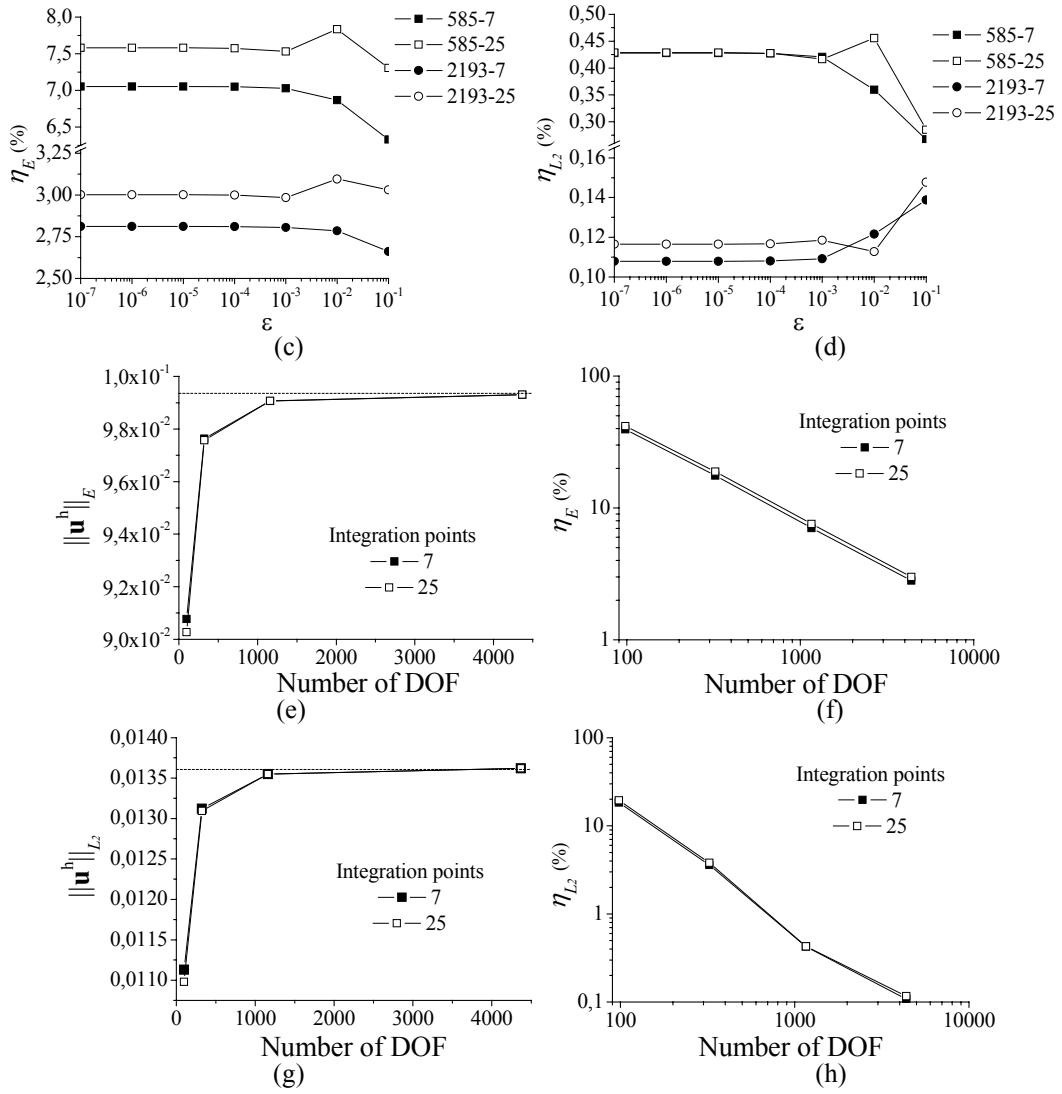


Figure 7 – Analysis results for the cantilever beam problem – a) $\beta \times \eta_E$, b) $\beta \times \eta_{L_2}$, c) $\epsilon \times \eta_E$, d) $\epsilon \times \eta_{L_2}$, e-f) Convergence: $\text{DOF} \times \|\mathbf{u}^h\|_E$ and η_E , g-h) Convergence: $\text{DOF} \times \|\mathbf{u}^h\|_{L_2}$ and η_{L_2} .

Figure 8 shows the displacement u_y at $x=0$ for the integration meshes in Fig. (6c) and (6d) with details at $y=0,25$. In this figure are used 7 integration points, $\epsilon=10^{-4}$ and $\beta=1.5$.

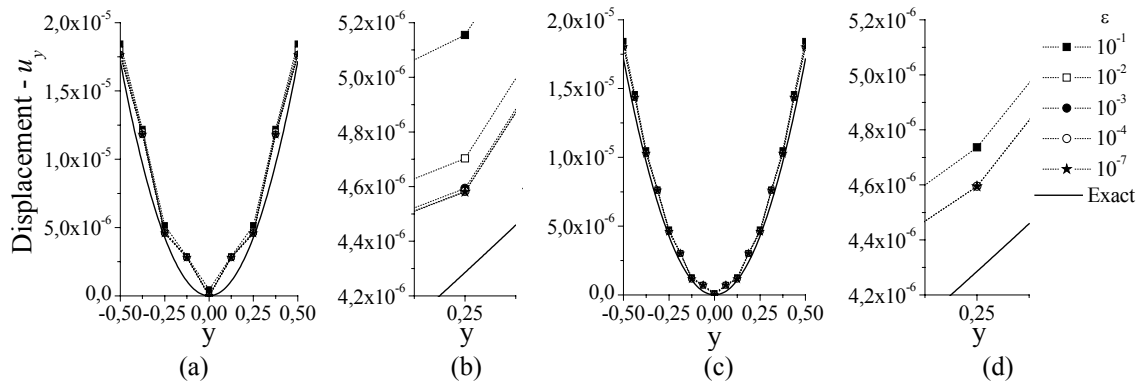


Figure 8. Displacement u_y at $x=0$: a) integration mesh 6c; b) detail at $y=0,25$; c) integration mesh 6d; d) detail at $y=0,25$.

4.2. Infinite plate with hole

In this example, we consider an infinite plate with a central hole as illustrated in Fig. (9), where we enforce the necessary symmetry conditions and impose, over the prescribed traction boundary of the finite plate, the exact traction distribution, obtained from the analytical solution presented by Timoshenko and Goodier (1970):

$$\sigma_{xx}(x,y) = 1 - \frac{a^2}{r^2} \left(\frac{3}{2} \cos 2\phi + \cos 4\phi \right) + \frac{3a^4}{2r^4} \cos 4\phi, \quad \sigma_{yy}(x,y) = -\frac{a^2}{r^2} \left(\frac{1}{2} \cos 2\phi - \cos 4\phi \right) - \frac{3a^4}{2r^4} \cos 4\phi, \quad (25)$$

$$\sigma_{xy}(x,y) = -\frac{a^2}{r^2} \left(\frac{1}{2} \sin 2\phi + \sin 4\phi \right) + \frac{3a^4}{2r^4} \sin 4\phi,$$

with $a=1$ to the case in Fig. (9).

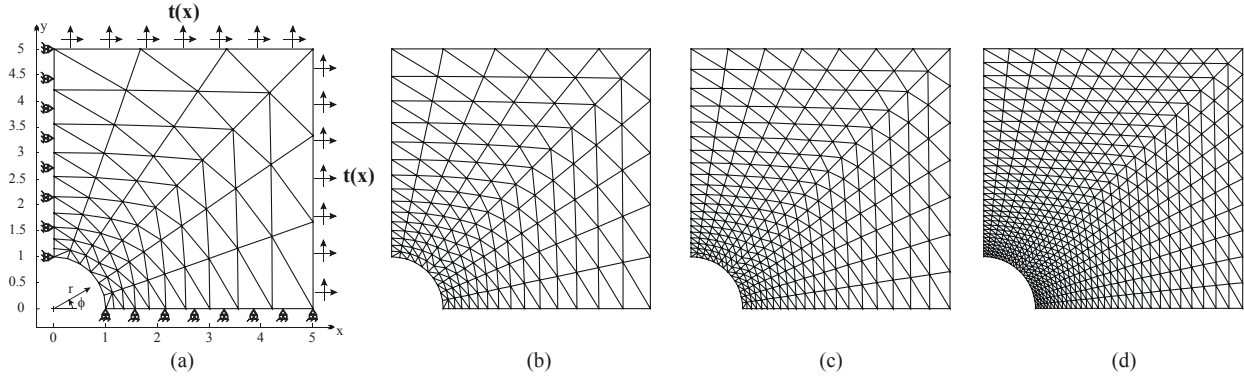


Figure 9. Infinite plate with hole model problem and integration meshes: a) integration mesh with 120 cells/77 nodes; b) 300 cells/176 nodes; c) 560 cells/315 nodes; d) 1200 cells/651 nodes

Again, the first investigation performed is the determination of an adequate value for the support size β . This analysis was performed considering the β change effect in η_E taken into account the integration meshes in Fig. (9c) and Fig. (9d) and considering $\varepsilon=10^{-4}$. This result is depicted in Fig. (10a). From this result it is possible to conclude, once more, that $\beta \cong 1.5$ is an adequate value. Figure (10b) shows the sensitivity study of the parameter ε upon η_E , for integration meshes in Fig. (9c) and Fig. (9d). Figures (10c) and (10d) shows the convergence aspects for integration meshes in Fig. (9a) to Fig. (9d). The dashed upper line in Fig. (10d) represent the exact energy norm for the proposed Infinite plate with hole model problem. In the Figures (10a) to (10c) the legend means the number of particles and the number of integration points.

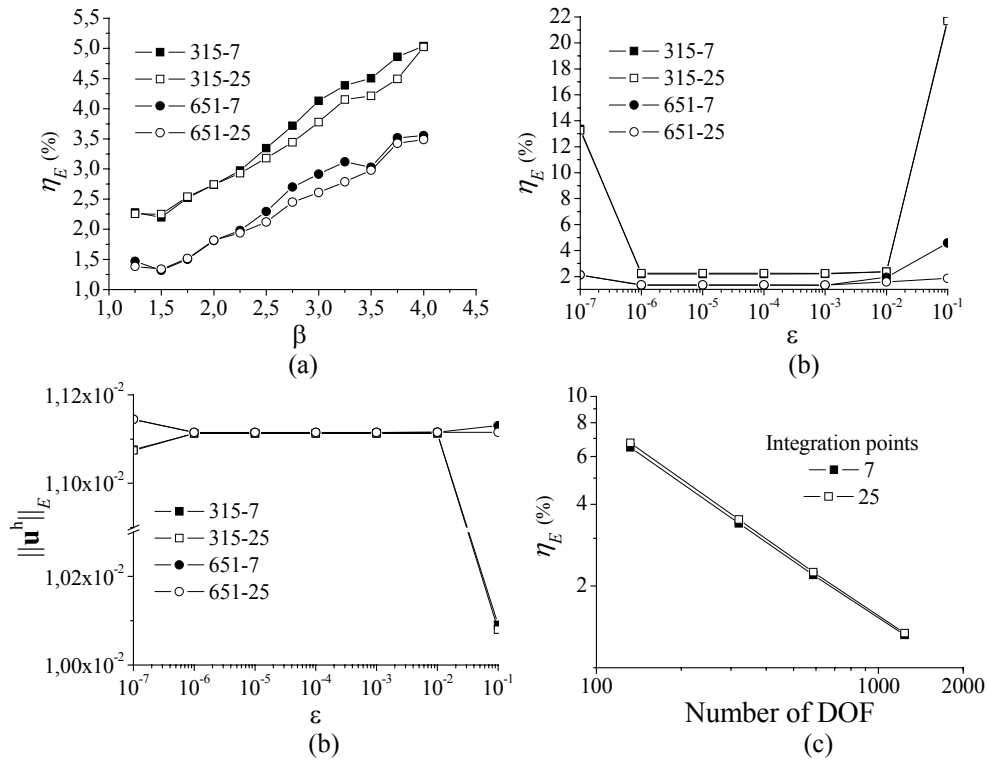


Figure 10. Analysis results for the infinite plate with hole problem – a) $\beta \times \eta_E$, b) $\varepsilon \times \eta_E$, d) Convergence: DOF \times $\|\mathbf{u}^h\|_E$, d) Convergence: DOF $\times \eta_E$.

5. Conclusions

In this paper is presented a modified element-free Galerkin that preserves the property of direct imposition of essential boundary conditions, as done in FEM. Numerical investigations were carried out in order to determine proper values for the support size β and suitable values for the range of perturbation parameter ε . To do so different integration meshes and problems are solved considering plane stress assumption inside the elastostatics theory.

From the results achieved it is possible to conclude that the values in relative error energy norm and in relative error displacement norm are stable for $\varepsilon \in [10^{-3}, 10^{-6}]$. For $\varepsilon > 10^{-3}$ we can verify an increase in the solution error due to the inappropriate enforcement of the essential boundary condition. On the other hand, for $\varepsilon < 10^{-7}$ we have experienced problems with respect to the ill conditioning of the moment matrix \mathbf{A} . Numerical investigations also lead to a support size value β around 1.5.

Such methodology is an outstanding alternative to impose the essential boundary conditions in mesh-free methods, and in special to the EFG method, and may be very promising when applied in nonlinear problems.

As a drawback of such procedure we can mention the loss of regularity of the shape functions when approaching the essential boundary and the EPUFE weight function dependence of an integration mesh.

6. Acknowledgements

We want to acknowledge the support of the CNPq – Conselho Nacional de Desenvolvimento Científico e Tecnológico – of Brazil. Grant Numbers: 470426/01-2 and 141806/2000-1.

7. References

- Alves, M.K. and Rossi, R., 2003, “A modified element-free Galerkin method with essential boundary conditions enforced by an extended partition of unity finite element weight function”, *Int. J. Numer. Meth. Eng.* Vol.57, pp. 1523-1552.
- Belytschko, T., Lu, Y.Y. and Gu, L., 1994, “Element-free Galerkin methods”, *Int. J. Numer. Meth. Eng.*, Vol.37, pp. 229-256.
- Belytschko, T., Organ, D. and Krongauz, Y., 1995, “A coupled finite element-element-free Galerkin method”, *Comput. Mech.*, Vol.17, pp. 186-195.
- Bugeda, G., 1991, “Estimación y corrección del error en el análisis estructural por MEF” (In Spanish), CIMNE Monograph n° 9, CIMNE, Barcelona, Spain.
- Duarte, A.C. and Oden, J.T., 1996, “An h-p adaptive method using clouds”, *Comput. Methods Appl. Mech. Engrg.*, Vol.139, pp. 237-262.
- Gu, Y.T. and Liu, G.R., 2001, “A coupled element free Galerkin/boundary element method for stress analysis of two-dimension solid”, *Comput. Methods Appl. Mech. Engrg.*, Vol.190, pp. 4405-4419.
- Hegen, D., 1996, “Element-free Galerkin methods in combination with finite element approaches”, *Comput. Methods Appl. Mech. Engrg.*, Vol.135, pp. 143-166.
- Huerta, A. and Méndez, S.F., 2000, “Enrichment and coupling of the finite element and meshless methods”, *Int. J. Numer. Meth. Eng.*, Vol.48, pp. 1615-1636.
- Kaljević, I. and Saigal, S., 1997, “An Improved Element Free Galerkin Formulation”, *Int. J. Numer. Meth. Eng.*, Vol.40, pp. 2953-2974.
- Krongauz, Y. and Belytschko, T., 1996, “Enforcement of essential boundary conditions in meshless approximations using finite elements”, *Comput. Methods Appl. Mech. Engrg.*, Vol.131, pp. 133-145.
- Lancaster, P. and Salkauskas, K., 1981, “Surfaces generated by moving least squares methods”, *Math. of Comput.*, Vol.37, pp. 141-158.
- Liu, W-K., Li, S. and Belytschko, T., 1997, “Moving least-square reproducing kernel methods (I) Methodology and convergence”, *Comput. Methods Appl. Mech. Engrg.*, Vol.147, pp. 113-154.
- Lu, Y.Y., Belytschko, T. and Gu, L., 1994, “A new implementation of the element-free Galerkin method”, *Comput. Methods Appl. Mech. Engrg.*, Vol.113, pp. 455-471.
- Melenk, J.M. and Babuška, I., 1996, “The partition of unity finite element method: basic theory and applications”, *Comput. Methods Appl. Mech. Engrg.*, Vol.39, pp. 289-314.
- Mukherjee, Y.X. and Mukherjee, S., 1997, “On boundary conditions in the element-free Galerkin method”, *Int. J. Numer. Meth. Eng.*, Vol.19, pp. 229-256.
- Timoshenko, S.P. and Goodier, J.N., 1970, “Theory of Elasticity”, 3rd edition. McGraw-Hill, New York.
- Ventura, G., 2002, “An augmented Lagrangian approach to essential boundary conditions in meshless methods”, *Int. J. Numer. Meth. Eng.*, Vol.53, pp. 825-842.